Experimental Design and Validation of an Adjustable Guide Grass Structure for a Grain Combine Harvester Thresher Based on a Material Movement Model

Luofa Wu *, Daogen Chen , Xieqing Xu , Yanqi Wu

Posted Date: 21 April 2023

doi: 10.20944/preprints202304.0678.v1

Keywords: Motion model; Grain combine harvester; threshing device; guide grass

Article

Experimental Design and Validation of an Adjustable Guide Grass Structure for a Grain Combine Harvester Thresher Based on a Material Movement Model

Wu Luofa [1], Xu Xieqing [1], Wu Yanqi [2] and Chen daogen [1]

[1] Institute of Agricultural Engineering, Jiangxi Academy of Agricultural Sciences, China
[2] Department of Electronic Engineering, Eindhoven University of Technology，Netherlands
* Correspondence: wyqjx001@mail.ustc.edu.cn

Abstract: Threshing device is the core component of grain combine harvester, and its working performance determines the working quality and production efficiency of the harvester to a great extent. The straw guide plate plays an important role in the threshing device to dredge the threshing matter and control the threshing time of the combine harvester matter in the threshing chamber. In the past, the guiding structure of threshing device could not optimize the working performance of the machine by adjusting the spiral angle, that is, most cereal combine harvester may not be fed smoothly or even clogged when operating under different crop types, yield differences and operating environments, a kind of threshing device with adjustable guide straw board was studied. In this study, the movement model of the straw on the straw guide plate was analyzed, and it was found that the spiral angle "α"of the straw guide was $0<\alpha<58°$.Three-factor and three-level response surface method was used to carry out field experiment on drum speed, working speed and guide grass plate spiral angle, and the experimental data were analyzed by quadratic polynomial regression.The results show that the drum speed, working speed and the spiral angle of the guide grass plate have significant effects on the loss rate (*PLR*) , impurity content (*PIR*) and breakage rate (*PBR*) , the drum speed and working speed have an interactive effect on the impurity ratio (*PIR*) , and the working speed and the helical angle of the guide grass plate have an interactive effect on the loss ratio (*PLR*) and breakage ratio (*PBR*) , there is an interaction between the rotary speed of the roller and the helical angle of the guide grass plate on the crushing rate (*PBR*) .Further optimization analysis showed that the predicted value was *PLR* = 1.18% , *PIR* = 0.72% , *PBR* = 0.53% , the experimental verification value was *PLR* = 1.26% , *PIR* = 0.73% , *PBR* = 0.61% . The absolute error between the experimental value and the predicted value was very small, however, the optimized field test verified value decreased by 8.31% , 50.04% and 60.30% respectively, which indicated that the optimized harvester had better operation quality, in particular, *PIR*, *PBR* and other two indicators have a greater increase in the effect.

Keywords: motion model; grain combine harvester; threshing device; guide grass

1. Introduction

Rice is one of the most important grain crops in China. Harvest is the last important link in rice production, and the realization of rice mechanized combine harvest is of great significance to improve production efficiency, reduce labor intensity and reduce harvest loss. Threshing device is the core component of grain combine harvester, and its working performance determines the working quality and production efficiency of the harvester to a great extent. There are many research directions of threshing device, and it is complex. The structure parameters, operation parameters and crop properties of threshing device will affect the threshing effect.

Chinese scholar Yang Fangfei and others used theoretical deduction combined with high-speed video to verify, they found that the grain in the concave side of the nail teeth by the strong impact of the grain tangential speed increased sharply, when the grain reaches the side of the cover plate, the grain moves in a spiral motion along the guide plate under the action of inertia force. On the other hand, during threshing, the threshing teeth contact directly with the crops, and the structure, stiffness

and moving speed of the threshing teeth have a direct impact on the threshing effect. Through contact theory, experimental analysis and finite element analysis, it is shown that the grain damage degree and crushing rate increase with the increase of the linear velocity of threshing teeth. The results show that the power consumption and impurity ratio of the threshing roller with short bar-plate teeth combination are better than that of the roller with nail teeth. In addition, Xie Fang studied the influence of the rigidity of the threshing teeth on the threshing performance, and found that the flexible threshing teeth can help to reduce the crushing rate and improve the seed germination rate. In addition, some scholars have studied the relationship between feeding amount and yield loss rate. The results show that the higher the feeding amount within a certain range, the higher the yield loss rate.

In recent years, the discrete element method and optimization test technique have become the important means in the research of harvester design. Noah. Tang used Edem to simulate the threshing process, and got the relationship of speed, track and time of rice straw movement. The results showed that in the axial threshing device, the average movement velocity of rice straw was 6.68 m/s, which was 34.06% of the circumferential velocity of the axial threshing drum. The relative error between simulation speed and test speed of threshing roller is 1.70% ~ 2.16% , and the relative error of straw movement time is 3.88% . Zhan Su and others used EDEM to analyze the influence of threshing and material transportation by different adjustment modes of threshing clearance. The simulation results show that the material separation and transportation capability is better by adjusting threshing clearance by roller than by adjusting concave sieve. On the other hand, Zhengzhong Zhang et al used response surface method to optimize the working parameters with multi-objective, taking drum speed, concave screen speed and feed chain speed as factors, when the drum speed is 547.6 r/min, the concave sieve speed is 0.93 m/s and the feed chain speed is 1.06 m/s, the predicted values of loss rate, breakage rate and impurity content rate are 1.95% , 0.29% and 0.58% , respectively, and the verification test and the forecast value are basically consistent. Zongwangyuan et al have shown that the function of the guide grass plate is mainly to transport the material in the threshing device from the roller feeding end to the grass discharging end smoothly, and the axial movement of the material mainly depends on the propelling function of the guide grass plate, the guide angle of straw guide has an important influence on the threshing time and whether the straw can be discharged from the threshing chamber.

To sum up, the movement and stress state of crops in the threshing device have a great influence on threshing performance, and the straw guide plate plays a role in the threshing device to dredge the threshing matter and control the threshing time of the threshing matter in the threshing room, it has a great influence on the loss rate, impurity content and breakage rate of combine harvester. When investigating the grass guiding structure of the threshing equipment, we can further find that the angle of the grass guiding structure of the existing grain combine harvester threshing equipment is mostly not adjustable, that is, most cereal combine harvester may not be fed smoothly or even clogged under different crop types, yield differences, and operating conditions In addition, a small number of combine harvester may control the threshing time in the threshing chamber by adjusting the installation angle of the straw guide plate, but they may also adjust the installation angle by dismantling the straw guide plate one by one, the operation procedure is complicated and the professional ability of personnel is required, or the whole adjustment method is adopted, but it is difficult to adjust the operation force, which is very inconvenient in the actual use. To this end, we have designed a new type of adjustable grass guide structure on the grain combine harvester threshing device. The spiral angle of the grass guide plate can be adjusted with a small operating force to control the threshing time of crops in the threshing chamber, in order to understand the influence of the parameters of the guide grass structure, such as the helix angle, working speed and drum rotation speed, on the working effect, and to improve the depuration rate of the harvester, the response surface optimization test was used to carry out the test and analysis of the new guide grass structure, reduce the loss rate of threshing.

Preprints (www.preprints.org) | NOT PEER-REVIEWED | Posted: 21 April 2023 doi:10.20944/preprints202304.0678.v1

2. Structure design and model analysis of grass guide

2.1. Overall structure of the harvester

Model 4LZ -4.0 harvester consists of chassis, rotary, cutting table, lifting device, threshing device, screening device, granary and so on. The overall structure is shown in Figure 1. The operation process is as follows: the rice enters the cutting table device under the guidance of the threshing wheel, the straw is cut off by the cutter and transported to the threshing device through the lifting device, and the separation of the grain and the straw is completed in the threshing device, then, the grain is cleaned by the screening device, and finally the grain is transported to the granary for temporary storage, so as to complete the mechanized harvesting of rice.

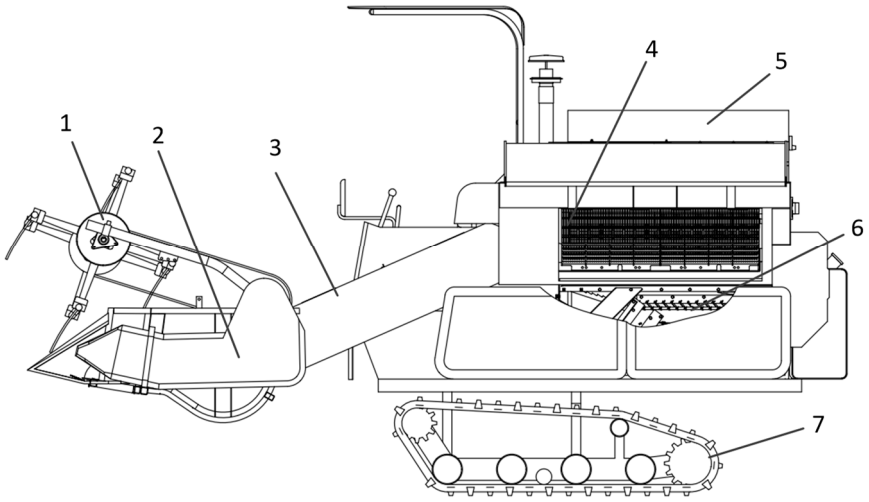

Figure 1. 4lz-4.0 longitudinal axial flow crawler harvester structure diagram. 1 Puller, 2 cutter, 3 lifting device, 4 threshing device, 5 granary, 6 screening device, and 7 chassis.

Table 1. 4LZ-4.0 Harvester main operating parameters.

Parameter	Value
Chassis power/(kW)	65
Machine size (length × width × height)/mm	5015×2560×2820
Weight of the whole machine/kg	2990
Working cut/mm	2000
Feeding amount/(kg·s^{-1})	4
Work efficiency/hm^2·h^{-1}	0.2~0.5

2.2. Threshing device and grass guiding structure

Threshing device is the core component of harvester, including Feed Inlet, drum assembly, grass guide structure, concave plate sieve, cover plate, etc. , the grass guiding structure is installed on the cover plate directly above the threshing drum, so that the crops can move smoothly in the threshing chamber. When the threshing device works, the rice is fed into the threshing separation chamber with the action of the forced feeding wheel, and the rice fed moves in the threshing separation chamber with the rotation of the threshing roller, and the threshing nail teeth of the high-speed rotation strike the rice mainly, under the action of rubbing, the rice grain separated from the stalk, and the rice stem moved along the roller axis under the action of the straw guide Under the action of centrifugal force, the seeds and some impurities, such as short stalks and light impurities, fall into the feeder box below.

The guide grass board on the market mostly uses the fixed type, namely the spiral angle of the guide grass board is the fixed value. The Type 4LZ-4.0 Harvester studied in this paper adopts a new type of threshing device with adjustable grass guide structure, as shown in Figures 2 and 3. The grass

Preprints (www.preprints.org) | NOT PEER-REVIEWED | Posted: 21 April 2023 doi:10.20944/preprints202304.0678.v1

guiding structure comprises a rotating shaft, an adjusting pull rod, a fixed grass guiding board (1 piece) , a main adjustable grass guiding board (1 piece) , a connecting rod and a follow-up adjustable grass guiding board (7 pieces) , the adjustable pull rod is connected with the main adjustable straw plate through the rotating shaft, and the main adjustable straw plate is connected with the follow-up adjustable straw plate through the connecting rod. Through the small operating force, the adjusting rod rotates, the rotating shaft drives the main adjustable guide grass plate to rotate, and then through the connecting rod drives the follow adjustable guide grass plate to rotate synchronously, thus realizing the adjustment of the guide grass plate spiral angle. Eight adjustable guide grass plates are used to control the flow velocity of crops during threshing process and improve the smoothness of threshing transportation. One fixed guide grass plate is fixed above the roller of the grass outlet, which can effectively guide the flow of weeds such as long stems.

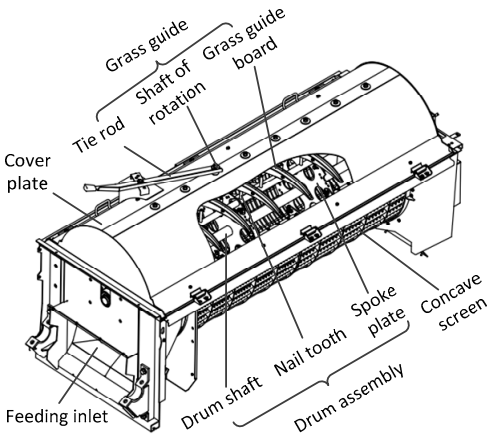

Figure 2. structure diagram of threshing device.

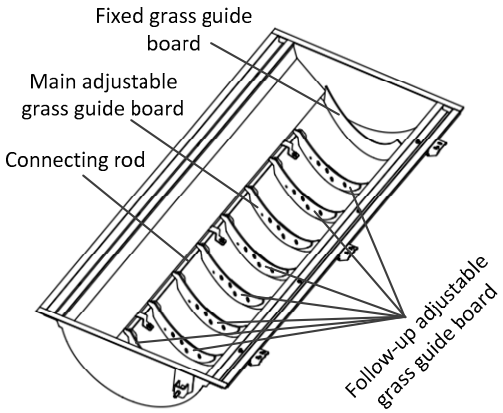

Figure 3. the structure and distribution of grass guiding device.

2.3. Analysis of mathematical model of material movement

In fact, the distribution of rice straw in the threshing device is loose, the straws are intertwined or clump, and the movement state has strong randomness. Therefore, it is very difficult to analyze the movement of straw on the guide structure. To facilitate the analysis of the problem, some assumptions and simplifications need to be made to the model:

Preprints (www.preprints.org) | NOT PEER-REVIEWED | Posted: 21 April 2023 doi:10.20944/preprints202304.0678.v1

2.3.1. Basic assumptions

(a)The straw was fed continuously and evenly without considering the effect of straw humidity on the flow

(b)The straw sticks to the cover board and flows continuously and uniformly along the guide grass board, without considering the mutual movement of the straw

(c)The rotation of the threshing drum can only push the straw, and does not change the speed of straw on the straw guide plate

(d)The crop is an inelastic body. When the crop is grasped by the threshing teeth, it moves at the linear speed of the roller without considering the change process of its acceleration.

2.3.2. Motion modeling

In the threshing process, the threshing drum rotates around the axis ω, and the distance between O-point and the axis of rotation is R. On the one hand, the straw particle at O-point rotates along the axis driven by threshing drum with traction velocity V_e, and on the other hand, the relative sliding speed between the straw particle and the grass guide plate is V_r, the velocity (absolute velocity) V_a of straw particle can be obtained by velocity triangle synthesis, as shown in Figure 4. According to the research of scholars, the relationship between the average velocity of straw movement and the circumferential velocity of threshing drum is a coefficient λ (the measured λ is 1/3 ~ 1/4) . Assuming that the rotating speed of the drum is V_o at the circumference and the average speed of straw at the guide grass plate relative to the drum (traction speed) is V_e, there are:

$$\begin{cases} V_o = \omega R \\ V_e = \lambda V_o \end{cases} \quad (1)$$

The velocity diagram is further refined, as shown in figure 5. Assuming that the friction coefficient between straw and straw is μ, the direction of the absolute velocity of straw particle and the normal direction of the straw guide are at an angle, Φ. the friction angle, then there are: $\mu=\tan(\Phi)$. α is the spiral rising angle of the guide grass plate. By using velocity decomposition and trigonometric variation, and taking into account the correlation between the correction coefficient something (something and crop characteristics, structural clearance, etc. , according to the experiment, ʒ; Something $0<ʒ<1$) , the following relationship can be obtained:

$$\begin{cases} V_a = \lambda ʒ \omega R \frac{sin\alpha}{cos\Phi} \\ V_r = \lambda ʒ \omega R(cos\alpha - \mu sin\alpha) \\ V_z = \lambda ʒ \omega R sin^2\alpha(cot\alpha - \mu) \end{cases} \quad (2)$$

In the upper model, the particle velocity of V_z straw is along the axial direction of the roller.In order to ensure the normal straw transportation, $V_z>0$. $Cot\alpha-\mu>0$. Further information:

$$A+\Phi<90° \quad (3)$$

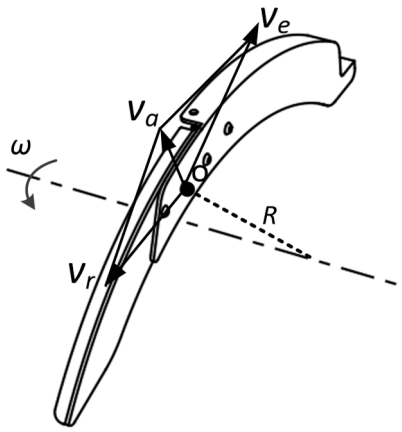

Figure 4. Velocity Triangle.

Preprints (www.preprints.org) | NOT PEER-REVIEWED | Posted: 21 April 2023 doi:10.20944/preprints202304.0678.v1

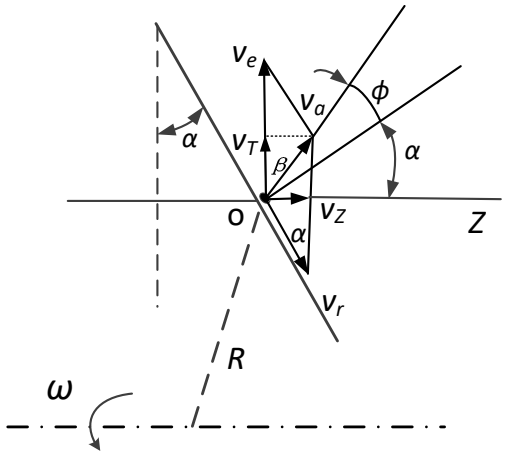

Figure 5. speed analysis detail diagram.

2.3.3. Movement model analysis

Further analysis of equation (2), According to the condition of product, the rotating speed of threshing drum is 600r/min, corresponding ω=40π/s, the diameter of threshing device is 600mm, corresponding R is 0.3 m, set λ=1/3、ʒ=1/2(λ、ʒ different amplitude, does not affect the trend) , then:

$$V_z = \lambda ʒ \omega R sin^2\alpha(cot\alpha - \mu) = 2\pi sin^2\alpha(cot\alpha - \mu) \quad (4)$$

The axial transport of straw under different μ values was compared by the upper model. According to scholars' research, crop humidity and friction coefficient myopia is a linear relationship, so set μ=0.2 to reflect the low moisture state of straw, set μ=1.0 to reflect the high moisture state of straw. The relationship between the spiral angle and the axial velocity of straw particle is analyzed, and the corresponding curve is shown in Figure 6.

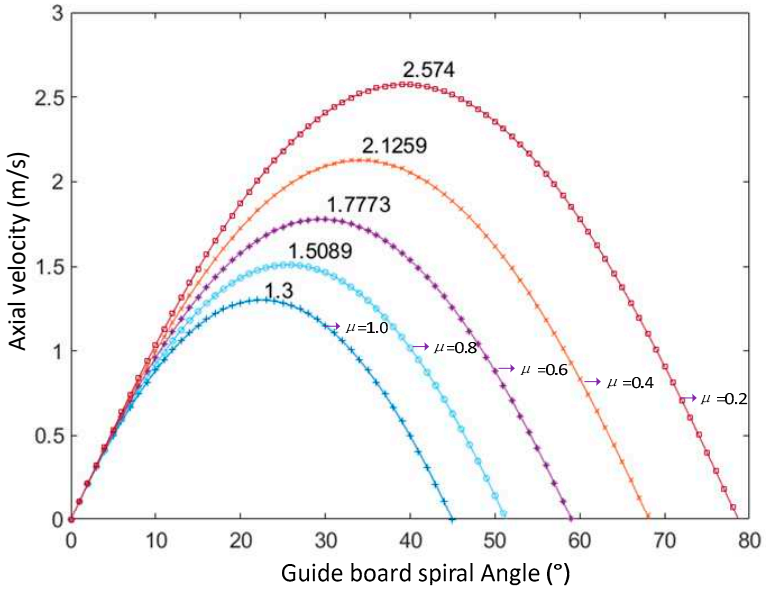

Figure 6. the curve of the axial velocity between the spiral angle and the straw particle under different μ.

It can be seen from Figure 6 that the relationship between the axial velocity of straw particle and the spiral angle of straw guide is an inverse parabola. When the spiral angle is small, the axial velocity of straw particle is small, the material flow is slow, and the threshing process of crop is long, although the separation is sufficient, with the increase of helix angle, the axial velocity of straw particle increases, the material flow speed increases, and the threshing process is short, which leads to

Preprints (www.preprints.org) | NOT PEER-REVIEWED | Posted: 21 April 2023 doi:10.20944/preprints202304.0678.v1

insufficient threshing and affects the threshing quality With the further increase of the spiral angle, the axial velocity of straw particle decreased after the peak value, and the conveying capacity decreased. On the other hand, when μ value decreases, the spiral angle corresponding to the peak value of the curve has an increasing trend, and the corresponding amplitude of the peak value of the curve also has an increasing trend.

According to "*the manual of agricultural machinery design*", the friction angle ϕ between rice and steel plate is from 23°~32° . According to Formula (3) , the value of spiral angle α should be $0<\alpha<58°$ to ensure the normal transportation of straw.

3. Verify materials and methods

3.1. Test equipment and materials

The experimental equipment includes adjustable straw-plate type 4LZ-4.0 harvester, fiber tape (length range 0-100m, accuracy 1mm) , Platform scales （Models：DH-E318, table surface 30cm × 40cm, accur1Gy 1g) , Electronic scales（Models：LD510-2, accuracy 0.01g) , electro-thermal constant temperature blast drying box （Models：E804-60A) , woven bag, 2 m × 1m sampling frame, standard and so on. The experiment site is located in the outdoor farm of Yujiang district, Yingtan, Jiangxi province. The rice variety is Jianyou 718.

Figure 7. diagram of test site.

3.2. Evaluation Index and test design

3.2.1. Evaluation Index

Based on standard NY T498-2013"Rice combine harvester, Operation Quality", the experiment was carried out, mainly considering three technical indicators: loss rate, impurity content rate and breakage rate.

1. Loss Rate (PLR) : rice was harvested in selected test areas and the total quality of harvested rice was recorded. After harvest, 5 points were selected in the rice field with the sampling frame, and the straw, residue and paddy on the ground were collected in the sampling frame, and the average value was taken after weighing. The loss rate is calculated according to the following formula:

$$PLR = \frac{m_s}{m_h+m_s} \times 100\% \quad (5)$$

Formula:*PLR* is the loss rate, the unit is percentage (%) ;

m_s is the loss of rice quality per square meter in g/m² units;

m_h is the quality of rice harvested per square meter in g/m²

2. Percentage of impurities (PIR): 5 random samples of rice harvested by harvester, each sample not less than 2000g, After cleaning and removing impurities, each sample is weighed, and the average value is obtained after calculating the impurity content according to the formula below:

$$PIR = \frac{m_z-m_q}{m_z} \times 100\% \quad (6)$$

In formula: *PIR* is impurity content, the unit is percentage (%) ;

m_z is sample mass in g;

m_q is sample mass in g after impurity removal

Preprints (www.preprints.org) | NOT PEER-REVIEWED | Posted: 21 April 2023 doi:10.20944/preprints202304.0678.v1

3. Crushing rate (PBR) : after the removal of impurities after the seed samples mixed, take 5 samples, each 100 g, pick out one of the broken, hulled (skin) of the seeds after weighing, according to the formula calculated crushing rate after taking the average value, the formula is:

$$PBR = \frac{m_y - m_p}{m_y} \times 100\% \quad (7)$$

Formula: *PBR* is broken rate, the unit is percentage (%) ;

m_y is sample quality in g;

m_p was the quality of the samples after the broken grains were cleared, and the unit was g

3.2.2. Test design

According to the previous research, the humidity, rotary speed, operating speed, stubble height, cutting width, threshing clearance and other factors have a greater impact on the harvest quality. Considering the focus of this study, under the certain condition of other structural parameters, the rotating speed (*A*) , operating speed (*B*) and the spiral angle (*C*) of the guide grass plate are selected as the experimental factors, the loss rate (*PLR*) , inclusion rate (*PIR*) and breakage rate (*PBR*) were used as evaluation indexes to design the test.

The harvest experiment was carried out in the same rice field to ensure the relative consistency of rice humidity and maturity. The average moisture content of rice straw was 28.63% , and the friction coefficient μ between straw and straw guide was about 0.64. It can be seen from Figure 6 that the axial velocity of straw particle is larger when the spiral angle of straw guide is in the range of 10°~50° . According to the working condition of the machine, 15° , 25° and 35° are selected to carry out the experiment, and the spiral angle of the guide grass plate is adjusted by rotating the adjusting rod.

Some scholars have shown that when stubble height and cutting edge are constant, the feeding quantity and working speed are approximately linear. In this experiment, fixed stubble height of 160mm, full-beam harvest, through the operation speed to achieve changes in the feeding rate, when the operation speed is too low, will affect the operation efficiency, when the operation speed is too high, it is easy to cause the jam of the threshing roller. The working speed of the threshing roller is 2.5 km/h, 3.5 km/h and 4.5 km/h. Drum speed can be directly adjusted to control the machine, drum speed is too low, easy to appear unclean threshing, drum speed is too high, easy to cause rice crushing, according to the working condition of the machine, the rotating speed of the drum is selected to carry out the experiment by 500r/min, 600r/min and 700r/min.

In order to reduce the number of field trials and take into account the number of factors, a three-factor, three-level response surface experiment was carried out with Box-Behnken central combined experiment design theory, and the experimental factors were coded as shown in Table 2.

Table 2. coding of trial factors.

	Levels		
Factors	-1	0	1
Drum speed（*A*,r/min）	500	600	700
Operation Speed（*B*,km/h）	2.5	3.5	4.5
Guide blade spiral angle（*C*,°）	15	25	35

4. Test results and analysis

4.1. Response Surface test results

According to the field test flow and evaluation index calculation method, the field test was carried out. The response surface test table and the corresponding test results are shown in Table 3. The average PLR, PIR and PBR of 17 treatments were 1.36% , 1.10% and 0.99% respectively.

Preprints (www.preprints.org) | NOT PEER-REVIEWED | Posted: 21 April 2023 doi:10.20944/preprints202304.0678.v1

Table 3. Results of field trials.

Serial number	Experimental factor			Evaluation indicators/%		
	A/(r/min)	*B*/(km/h)	*C*/(°)	*PLR*	*PIR*	*PBR*
1	500	3.5	35	1.64	0.65	0.52
2	700	3.5	35	1.34	1.30	1.18
3	700	2.5	25	1.23	1.47	1.52
4	600	3.5	25	1.11	0.89	0.73
5	600	2.5	35	1.34	1.02	0.62
6	600	4.5	35	2.04	1.25	1.10
7	600	3.5	25	1.14	0.94	0.68
8	500	3.5	15	1.49	0.85	0.74
9	600	4.5	15	1.58	1.34	1.23
10	600	3.5	25	1.03	0.97	0.70
11	600	3.5	25	1.08	0.86	0.63
12	500	2.5	25	1.42	0.70	0.82
13	600	2.5	15	1.26	1.27	1.16
14	500	4.5	25	1.99	1.13	1.05
15	600	3.5	25	0.99	0.83	0.75
16	700	3.5	15	0.83	1.53	1.72
17	700	4.5	25	1.69	1.62	1.68

4.2. Significance analysis

Design-Expert software is a universal multi-functional mathematical statistics and mathematical model processing software system. It integrates the functions of numerical calculation, statistical analysis, surface simulation and response surface analysis. In this paper, the data processing system of Design-Expert software is used to analyze the field test results (Table 3) . The results of significance test are shown in table 4.

Table 4. ANOVA of the regression model[a].

Indicator	Source	Sum of squares	df	Mean squares	F-value	P-value	Significance
PLR	Model	1.81	9	0.2	32.06	< 0.0001	**
	A	0.26	1	0.26	41.79	0.0003	**
	B	0.53	1	0.53	83.52	< 0.0001	**
	C	0.18	1	0.18	28.62	0.0011	**
	AB	3.03E-03	1	3.03E-03	0.48	0.5103	
	AC	0.032	1	0.032	5.15	0.0575	
	BC	0.036	1	0.036	5.74	0.0478	*
	A^2	0.084	1	0.084	13.36	0.0081	**
	B^2	0.58	1	0.58	92.27	< 0.0001	**
	C^2	0.054	1	0.054	8.66	0.0216	*
	Residual	0.044	7	6.29E-03			
	Lack of Fit	0.029	3	9.81E-03	2.69	0.182	

Preprints (www.preprints.org) | NOT PEER-REVIEWED | Posted: 21 April 2023 doi:10.20944/preprints202304.0678.v1

	Pure Error	0.015	4	3.65E-03			
	Cor Total	1.86	16				
	R^2	0.9763					
	Adj R^2	0.9459					
PIR	Model	1.37	9	0.15	43.35	< 0.0001	**
	A	0.84	1	0.84	239.53	< 0.0001	**
	B	0.097	1	0.097	27.65	0.0012	**
	C	0.074	1	0.074	21.17	0.0025	**
	AB	0.02	1	0.02	5.60	0.0499	*
	AC	2.25E-004	1	2.25E-004	0.064	0.8072	
	BC	6.4E-003	1	6.4E-003	1.83	0.2184	
	A^2	0.04	1	0.04	11.38	0.0119	*
	B^2	0.23	1	0.23	66.28	<0.0001	**
	C^2	0.032	1	0.032	9.16	0.0192	*
	Residual	0.025	7	3.501E-03			
	Lack of Fit	0.011	3	3.808 E-03	1.16	0.4268	
	Pure Error	0.013	4	3.27E-03			
	Cor Total	1.39	16				
	R^2	0.9824					
	Adj R^2	0.9597					
PBR	Model	2.29	9	0.25	71.44	< 0.0001	**
	A	1.10	1	1.10	309.91	< 0.0001	**
	B	0.11	1	0.11	31.04	0.0008	**
	C	0.26	1	0.26	71.84	< 0.0001	**
	AB	1.225E-003	1	1.225E-03	0.34	0.5758	
	AC	0.026	1	0.026	7.20	0.0314	*
	BC	0.042	1	0.042	11.81	0.0109	*
	A^2	0.36	1	0.36	100.22	< 0.0001	**
	B^2	0.33	1	0.33	91.79	< 0.0001	**
	C^2	0.011	1	0.011	3.08	0.1228	
	Residual	0.025	7	3.558E-03			
	Lack of Fit	0.016	3	5.108E-03	1.43	0.1993	
	Pure Error	8.68 E-003	4	2.17E-03			
	Cor Total	2.31	16				
	R^2	0.9892					
	Adj R^2	0.9754					

[a]WhenP<0.01, extremely significant, symbolized with "**". When P < 0.05, significant, symbolized with "*".

As can be seen from table 4, *PLR* model significance test p < 0.01, *PLR* de-fit test p = 0.182, *PIR* model significance test p < 0.01, *PIR* de-fit test p = 0.4268, *PBR* de-fit test p < 0.01, the loss-of-fit test of *PBR* (p = 0.1993) showed that the quadratic regression equation test of *PLR*, *PIR* and *PBR* was highly significant, which indicated that the three models had a good fit in the experimental range, it can be

Preprints (www.preprints.org) | NOT PEER-REVIEWED | Posted: 21 April 2023 doi:10.20944/preprints202304.0678.v1

used to analyze and predict the effect of the three factors: drum speed (A) , working speed (B) and the spiral angle (C) .

The quadratic polynomial regression model derived from the regression coefficients calculated by Design-Expert software is as follows:

$$\begin{cases} PLR = 1.07 - 0.18A + 0.26B + 0.15C - 0.028AB + 0.09AC + \\ \qquad 0.095BC + 0.14A^2 + 0.37B^2 + 0.11C^2 \\ PLR = 1.07 - 0.18A + 0.26B + 0.15C - 0.028AB + 0.09AC + \\ \qquad 0.095BC + 0.14A^2 + 0.37B^2 + 0.11C^2 \\ PBR = 0.7 + 0.37A + 0.12B - 0.18C - 0.018AB - 0.08AC + \\ \qquad 0.1BC + 0.29A^2 + 0.28B^2 + 0.051C^2 \end{cases} \quad (8)$$

Formula: A—Drum speed code value

B—Code value for job speed

C—Guide grass plate spiral angle coding value

The **P** value of each factor was observed in table 4 that A, B, C, A^2, B^2 had significant effect on PLR ($p < 0.01$) , BC, C^2had significant effect on PLR ($p < 0.05$) , AB, AC had no significant effect on PLR ($P > 0.05$) . For PIR, the effects of A, B, C and B^2 were very significant ($p < 0.01$) , and those of AB, A^2 and C^2 were significant ($p < 0.05$) , while those of BC and AC were not significant ($P > 0.05$) . For PBR, the effects of A, B, C, A^2 and B^2 were very significant ($p < 0.01$) , while those of AC and BC were significant ($p < 0.05$) , while those of AB and C 2 were not significant ($P > 0.05$) .

The F-value of each influencing factor in table 4 was analyzed, and the larger the F-value was, the greater the influence on the response index was. Therefore, the order of single factor effect on PLR is as follows: working speed > drum speed > grass guide plate spiral angle, and the order of single factor effect on PIR is as follows: drum speed > working speed > grass guide plate spiral angle, the order of single factor effect on PBR was as follows: rotary speed of roller > spiral angle of guide grass > working speed.

For PLR interaction terms, the order of influence is: working speed × guide grass plate spiral angle > drum rotation speed × guide grass plate spiral angle > drum rotation speed × working speed, for PIR interaction terms, the order of influence is: drum rotation speed × working speed > working speed × grass guide plate spiral angle > drum rotation speed × grass guide plate spiral angle, for PBR, the Order of influence on the interaction terms was: working speed × draft guide plate spiral angle > drum rotation speed × draft guide plate spiral angle > drum rotation speed × working speed.

4.3. Response surface analysis

To visualize the interaction effect of two factors on the response, a 3D graph of the interaction effect between two factors can be created. Response surface and contour plots are usually generated for each fitting model as a function of two independent variables, with the other variables kept at the center. The obtained *PLR*, *PIR*, and *PBR* response surfaces are shown in Figures 8–10, respectively.

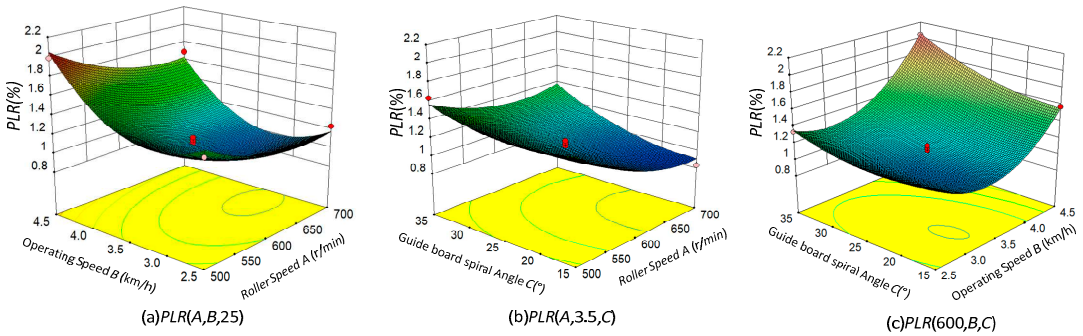

Figure 8. response surface and contour plot of *PLR*.

Figure 8 shows the response surface and contour plot for the loss rate (PLR) . As can be seen from Figures 8(a) and 8(b) , the loss rate (PLR) tends to decrease with the increase of drum speed (A) . This is because the roller speed (A) increases, the impact force of threshing teeth on straw increases,

Preprints (www.preprints.org) | NOT PEER-REVIEWED | Posted: 21 April 2023 doi:10.20944/preprints202304.0678.v1

the probability of impact per unit time also increases, the grain on straw is easier to be depurated, and the entrainment loss decreases. As can be seen from Figures 8(a) and 8(c) , the loss rate (*PLR*) first decreases and then increases as the operating speed (*B*, the corresponding feeding amount) increases, the number of straws entering the threshing drum per unit time was less, the rubbing action between straws was weakened, the grain was not threshed, and the loss rate was increased. On the contrary, when the operating speed is high, the unit time into too much straw, entrainment loss increases, loss rate also increases. As can be seen from Figures 8(b) and 8(c) , the loss rate (*PLR*) tends to increase gradually with the increase of the guide-blade helix angle (*C*) , which is due to the increase of the guide-blade helix angle, the time of straw threshing in the threshing drum is shortened, and the loss rate will increase if the grain is not completely threshed.

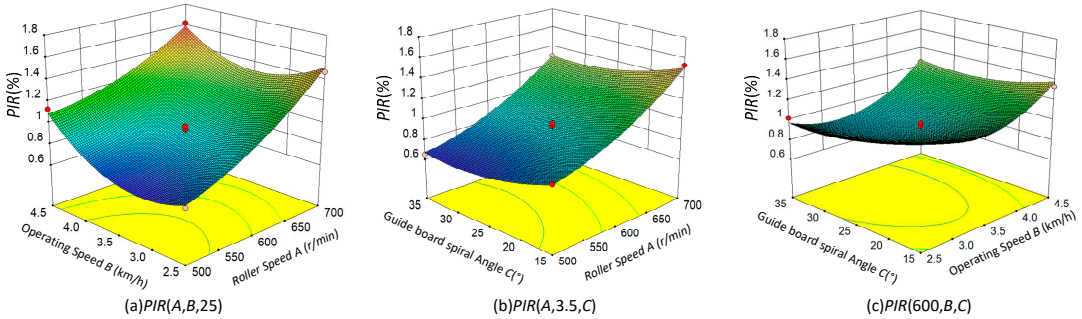

Figure 9. response surface and contour plot of *PIR*.

Figure 9 shows the response surface and contour plot of the impurity ratio (*PIR*) . As can be seen from Figure 9(a) and Figure 9(b) , the impingement ratio (*PIR*) tends to increase with the increase of drum speed (*A*) , because the impact force of threshing teeth on straw increases with the increase of drum speed (*A*) , the more the straw is crushed, the higher the impurity content is. As can be seen from Figures 9(a) and 9(c) , as the operating speed (*B*, the corresponding feeding amount) increases, the impurity ratio (*PIR*) first decreases and then increases, the probability of being beaten and crushed by threshing teeth is high, resulting in high impurity content. On the other hand, when the operating speed is high, the threshing roller has more straws, the corresponding threshing teeth are also more crushed straws, inclusion rate is large. As can be seen from Figures 9(b) and 9(c) , there is a decreasing trend in the percentage of impurities (*PIR*) with the increase of the guide-plate helix angle (*C*) , which is due to the increasing of the guide-plate helix angle, the time of straw threshing in the threshing drum is shortened, the time and times of straw beating are reduced, the straw is not easy to be crushed, and the impurity content is reduced.

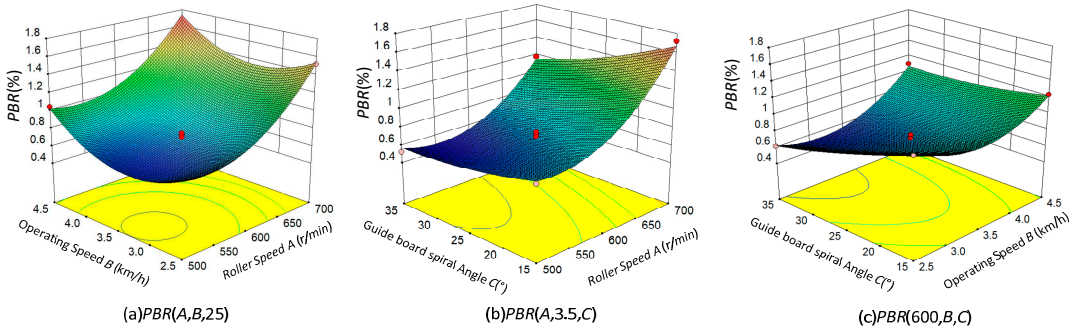

Figure 10. response surface and contour of *PBR*.

Figure 10 shows the response surface and contour plot of the crushing rate (*PBR*) . As can be seen from Figures 10(a) and 10(b) , the crushing rate (*PBR*) tends to increase with the increase of drum speed (*A*) , because the impact force of threshing teeth on grains increases with the increase of drum speed (*A*) , grain is easily broken, resulting in increased crushing rate. As can be seen from Figures 10(a) and 10(c) , the crushing rate (*PBR*) first decreased and then increased with the increase of the operating speed (*B*, corresponding feeding amount) , the probability of grain being crushed by

threshing teeth is high, resulting in high crushing rate. On the other hand, when the operating speed is high, the threshing drum of more grains, corresponding to the threshing teeth hit more grains, crushing rate is large. As can be seen from Figures 10(b) and 10(c) , there was a decreasing trend in the rate of breakage (*PBR*) with the increase of the guide-plate spiral angle (*C*) , which was due to the increasing of the guide-plate spiral angle, the time of straw threshing in the threshing drum was shortened, the time and times of grain beating were reduced, and the crushing rate was reduced.

4.4. Parameter optimization

Loss Rate (*PLR*) , inclusion rate (*PIR*) and crushing rate (*PBR*) are important indexes of harvester performance. The smaller the three indexes are, the better the harvester performance is. The optimization analysis can be carried out by using the optimization function of Design-Expert software in order to get better parameter combination. The constraints and results of the optimization are shown in Table 5.

Table 5. Constraints and solutions.

Name	Constraints						Solutions	
	Goal	Lower limit	Upper limit	Lower weight	Upper weight	Importance	Optimized results	Parameter adjustment
A(r/min)	is in range	500	700	1	1	3	551.29	550
B(km/h)	is in range	2.5	4.5	1	1	3	3.14	3
C(°)	is in range	10	50	1	1	3	28.22	28
PLR(%)	minimize	0	2	1	1	3	1.18	1.26
PIR(%)	minimize	0	1.60	1	1	3	0.72	0.73
PBR(%)	minimize	0	1.72	1	1	3	0.53	0.61

4.5. Validation tests

As shown in Table 5, taking into account the adjustable conditions of the harvester parameters, some adjustments are made to the recommended values of the optimized parameters. The rotating speed of the drum (*A*) is 550 r/min, and the operating speed (*B*) is 3 km/h, the field verification test was carried out by taking the helix angle (*C*) of grass guide plate at 28 ° for two times.The results show that the predicted value of the optimized *PLR* is 1.18% , the verified value is 1.26% , the relative error is 6.78% , and the absolute error is 0.08% , however, the field loss rate (*PLR*) of 17 treatments decreased by 8.31% .After optimization, the predicted *PIR* value was 0.72% , the verified *PIR* value was 0.73% , the relative error was 1.39% , the absolute error was 0.01% , but the verified *PIR* value was 50.04% lower than the average *PIR* value of the original 17 treatments.After optimization, the *PBR* predicted value was 0.53% , the PBR verified value was 0.61% , the relative error was 15.09% , the absolute error was 0.08% , but the *PBR* verified value was 60.30% lower than the field average value of the original 17 treatments.From the optimization results, the relative error of some indexes is large, but the absolute error is not high in general and the values of the three indexes are low.

5. Research conclusions and discussion

5.1. Conclusion

（1）In the threshing chamber, the straw guide plate plays an important role in dispersing and controlling the threshing time of the combine harvester, and has a great influence on the rate of seed purification and loss of threshing.To improve the suitability of grain combine harvester for different crop types, different yield differences and different operating environments, and to address the possibility of poor or even blocked feeding of crops, in this paper, a kind of longitudinal-axis adjustable spiral-angle grass guide structure and its threshing device are used to analyze the

movement mathematical model of the material on the grass guide plate, and the motion equation of the straw on the grass guide plate along the axis of the threshing roller is obtained, the equation shows that the axial velocity of straw particle has an inverse parabola relationship with the spiral angle of the straw guide.Considering the effect of humidity on the motion equation, the results show that the peak value and the helix angle of the equation decrease with the increase of humidity, which shows that the higher the humidity is, the lower the axial velocity of straw transportation is. In order to ensure the normal transportation of straw, the value of spiral angle α of straw guide plate should be $0<\alpha<58°$.

（2）Design-expert was used to design and analyze the three-factor and three-level response surface test for drum speed, operating speed and guide-blade spiral angle. The results show that the drum speed, working speed and the spiral angle of the guide grass plate have significant effects on the three performance indexes of *PLR*, *PIR* and *PBR*.Among them, the order of single factor to *PLR* is: working speed > drum speed > guide grass plate spiral angle, and the order of single factor to *PIR* is: drum speed > working speed > guide grass plate spiral angle, the order of single factor effect on *PBR* was as follows: rotary speed of roller > spiral angle of guide grass > working speed.For *PLR*, the order of influence of interaction terms is: working speed × guide grass plate spiral angle > drum rotation speed × guide grass plate spiral angle > drum rotation speed × working speed; For *PIR* interaction terms, the order of influence is: drum speed × working speed > working speed × grass-guide plate spiral angle > drum speed × grass-guide plate spiral angle; For *PBR*, the Order of influence on the interaction terms was: working speed × draft guide plate spiral angle > drum rotation speed × draft guide plate spiral angle > drum rotation speed × working speed.

（3）The optimized parameters were set as A=550 r/min, B=3 km/h and C=28° by using the optimization function of Design-Expert software. The results were as follows: *PLR* = 1.26% , *PIR* = 0.73% , *PBR* = 0.61% . The absolute error between the experimental value and the predicted value is very small, but the verified value of the optimized field experiment is 8.31% , 50.04% , 60.30% lower than the average value of the original 17 treatments field experiment, respectively, the results show that the response surface test model and the optimized parameters are applicable, and the optimized harvester has better operation quality, especially, *PIR* and *PBR* can be improved greatly.

5.2. Discussion

（1）Humidity directly determines the friction coefficient μ between straw and straw guide, and has a great influence on the loss rate, impurity content and breakage rate of grain combine harvester, it is also of great research value whether the influence of rice humidity on harvest effect can be eliminated by adjusting the angle of straw guide board.However, due to the difficulty in controlling rice humidity in grain combine harvester trials, this study did not take it as an independent factor to participate in field validation trials and optimization, and if it was a four-factor, three-level trial, there are too many experimental groups, and the observation and statistics are difficult. There may also be many problems in the Operability and practical application of field experiments.

（2）The effects of rice varieties, material characteristics and agronomy on threshing equipment were not fully considered in this experiment, to conduct field trials of adjustable grass guiding structure and threshing device under different crop types, different yield differences and different operating environments, the next step for the research team will be to explore the effects of different experimental factors on grain combine harvester loss rate, impurity content and crushing rate.

（3）With the development of science and technology, electromechanical and hydraulic control, sensors, Internet + , machine vision, computer simulation and other technologies are also widely used in combine harvester research. Advanced technology will inevitably bring complex structure, increase manufacturing costs, high temperature and high humidity operating environment also affect the service life of equipment. How to balance the ease of operation, the stability of use and the economy of purchasing machines will also be a key issue for both combine harvester and farmers to seriously consider.

References

1. Kang Jiaxin, Wang Xiushan, Xie Fangping, et al. Design and experiment of symmetrical adjustable concave for soybean combine harvester[J]. *Transactions of the Chinese Society of Agricultural Engineering (Transactions of the CSAE)*, 2022, 38(2): 11-22. (in Chinese with English abstract)
2. Fu J, Chen Z, Han L J, Ren L Q. Review of grain threshing theory and technology. *Int J Agric & Biol Eng*, 2018; 11(3): 12–20.
3. Tang Zhong, Li Yaoming, Xu Lizhang. Design and optimization for length of longitudinal-flow threshing cylinder of combine harvester[J]. *Transactions of the Chinese Society of Agricultural Engineering (Transactions of the CSAE)*, 2014, 30(23): 28－34. (in English with Chinese abstract)
4. Yang Fangfei, Yan Chuliang, Yang Bingnan, Yi Shujuan, Jiang Nan. Simulation and testing of cereal motion in threshing unit of combine harvester with axial feeding. *Transactions of the Chinese Society for Agricultural Machinery*, 2010, 41(12): 67-71, 88.
5. Xu Lizhang, Li Yaoming, Ding Linfeng. Contacting mechanics analysis during impact process between rice and threshing component[J]. *Transactions of the CSAE*, 2008,24(6)：146－149. (in Chinese with English abstract)
6. Xu Lizhang, Li Yaoming, Li Hongchang. Analysis on factors affecting performance of rice kernel damage during threshing. *Transactions of the Chinese Society for Agricultural Machinery*, 2008, 39(12): 55-59.
7. Xu Lizhang, Li Yaoming, Ma Zheng, Zhao Zhan, Wang Chenghong. Theoretical analysis and finite element simulation of a rice kernel obliquely impacted by a threshing tooth.[J]. *Biosystems Engi*neering, 2013, 114(2):146-156.
8. Li Yaoming, Li Hongchang, Xu Lizhang. Comparative experiments on threshing performance between short-rasp-bar tooth cylinder and spike tooth cylinder[J]. *Transactions of the CSAE*, 2008,24(3)：139-142.(in Chinese with English abstract)
9. Xie Fangping, Luo Xiwen, Lu Xiangyang, et al. Threshing principle of flexible pole-teeth roller for paddy rice[J]. *Transactions of the CSAE*, 2009,25(8)：110－114.(in Chinese with English abstract)
10. Xie Fangping, Luo Xiwen, Su Aihua, Wu Mingliang. Contrastive experiment on threshing by using rigid wire-loop,rigid pole tooth and flexible pole tooth. *Journal of Hunan Agricultural University (Natural Sciences)*, 2005, (6): 648-651.
11. Chen Du, Wang Shumao, Kang Feng, et al. Mathematical model of feeding rate and processing loss for combine harvester[J]. *Transactions of the CSAE*, 2011, 27(9): 18－21. (in Chinese with English abstract)
12. S. B. Andrews,T. J. Siebenmorgen,E. D. Vories, et al. Effects of Combine Operating Parameters on Harvest Loss and Quality in Rice[J]. *Transactions of the ASAE*, 1993, 36(6): 1599-1607.
13. Tang Z, Li Y, Xu L. Numerical simulation and test analysis of straw movement in threshing and separation unit[J]. *International Agricultural Engineering Journal*, 2014, 23(2): 35-42.
14. Su Zhan, Li Yaoming, Dong Yunhua , Tang Zhong, Liang Zhenwei. Simulation of rice threshing performance with concentric and non-concentric threshing gaps[J]. *Biosystems Engineering*, 2020, 197(1).
15. Liu Z, Dai S, Tian L, et al. Design and performance test of rotary grate concave threshing and separating unit of head-feeding combine harvester[J]. *Applied Engineering in Agriculture*, 2018, 38(2): 303-312.
16. Xie Gan.(2020) Design and experimental research of drum-shaped rod-tooth longitudinal axial flow threshing and separating device. MS thesis. Wuhan. Hubei Province. Huazhong Agricultural University.
17. Yang Fangfei, Yan Chuliang. Movement analysis of cereal in axial flow threshing roller space[J]. *Transactions of the Chinese Society for Agricultural Machinery*, 2008, (11): 48-50, 25.
18. Jin Xiaoliang, Zhu Xiaoxing, Jin Chengqian, Cao Guangqiao. Research on the power consumption model of grain threshing cylinder[J]. *Journal of Chinese Agricultural Mechanization,* 2015, 36(3): 30-33, 38.
19. M. A. Al-Mahasneh,T. M. Rababah. Effect of moisture content on some physical properties of green wheat[J]. *Journal of Food Engineering*, 2007, 79(4): 1467-1473.
20. Zhang Xiaoan. 2014. *Agricultural Machinery Design Manual*. Beijing : China Agricultural Science and Technology Press.
21. Agricultural industry standard of the P. R. China.(2013). NY/T 498-2013: Operating quality for rice combine harvesters. Lan Xinmin, et al.
22. Qiu Yibing.2008. *Test design and data processing.* Beijing : University of Science and Technology of China Press.
23. Wang F, Ma S, Ke W, et al. Optimization of basecutter structural parameters for under-the-ground sugarcane basecutting[J]. *Applied Engineering in Agriculture*, 2021, 37(2): 233-242.
24. Yang Guang, Chen Qiaomin, Xia Xianfei, et al. Design and optimization of the key components for 4DL-5A faba bean combine harvester[J]. *Transactions of the Chinese Society of Agricultural Engineering (Transactions of the CSAE)*, 2021, 37(23): 10-18. (in Chinese with English abstract)
25. Zongwang Yuan. Research on longitude axial flow threshing and separting unit of rape combing harvester. *Huazhong Agricultural University*. 2013
26. Peng Yuxing. Design and Experiment of the longitudinal axial threshing device for rice. *Hunan Agricultural University*, 2016

27. Wang Chery. Research on intelligent design method of threshing device of Rice Combine Harvester. *Jiangsu University*, 2020